SPLIT HYPERPLANE SECTIONS ON SMOOTH POLARIZED $K3$-SURFACES

ALEX DEGTYAREV

Abstract. We study hyperplane sections of smooth polarized $K3$-surfaces that split into unions of lines. We describe the dual adjacency graphs of such sections and find sharp upper bounds on their number. In most cases (starting from degree 6), we also compute all configurations of such sections.

1. Introduction

Virtually every known proof (*cf.* [19, 16, 6]) of Segre's celebrated theorem [19] on at most 64 lines on a smooth quartic surface $X \subset \mathbb{P}^3$ contains, as an essential part, the following argument: consider a plane section of X split into four lines $\ell_1, \ldots, \ell_4$; each of ℓ_i intersects at most 18 lines and every line not in the plane intersects exactly one of ℓ_i; hence, the number of lines is at most $4 \cdot (18 - 3) + 4 = 64$. In other words, proofs make an essential use of the plane sections of X that split into lines; in the dual adjacency graph of lines on X, the so-called *Fano graph* $\operatorname{Fn} X$, they are fragments isomorphic to the complete graph $K(4)$. (The proofs differ in their approach to the configurations of lines that do *not* contain a $K(4)$-fragment and in their treatment of the very special lines that intersects more that 18 others: the so-called *lines of the second kind* may have valency up to 20, *cf.* [15].)

Likewise, many papers dealing with lines on sextic $K3$-surfaces $X \subset \mathbb{P}^4$ make an extensive use of the split hyperplane sections of X. Recall that $X = Q_2 \cap Q_3$ is a regular complete intersection of a quadric and a cubic. A general hyperplane H intersects Q_2 in a quadric $\mathbb{P}^1 \times \mathbb{P}^1 \subset \mathbb{P}^3$, on which Q_3 cuts a curve C of bi-degree $(3, 3)$. If C splits into lines, it must consist of six generatrices, three from each of the two rulings, resulting in the complete bipartite graph $K(3, 3) \subset \operatorname{Fn} X$.

These observations lead us to the following natural question.

Problem 1.1 (I. Dolgachev [5])**.** What is the maximal number of

(1) $K(4)$-fragments in the Fano graph of a smooth quartic $X \subset \mathbb{P}^3$?
(2) $K(3, 3)$-fragments in the Fano graph of a smooth $K3$-sextic $X \subset \mathbb{P}^4$?

Certainly, similar questions can be asked for $2d$-polarized $K3$-surfaces $X \subset \mathbb{P}^{d+1}$.

To begin with, observe that a hyperplane section of a surface of degree $2d$ is a curve of degree $2d$ and, should it split into lines, there must be $2d$ of them. On the other hand, due to [2], the maximal number of lines on a $2d$-polarized $K3$-surface tends to decrease, oscillating between 24 and 21 when $2d \gg 0$. We show that split hyperplane sections (for short, *h-fragments*) do not exist if $2d > 28$.

2010 *Mathematics Subject Classification.* Primary: 14J28; Secondary: 14N25.
Key words and phrases. $K3$-surface, hyperplane section, Fano graph.
The author was partially supported by the TÜBİTAK grant 123F111.

Next, before addressing Problem 1.1 in its general form, one needs to understand the combinatorial structure of h-fragments as abstract graphs. The straightforward geometric description as in degrees 4 and 6 seems no longer available and, to our surprise, we discover that, more often than not, this graph is not unique. Even in degree $2d = 6$ the quadric surface $H \cap Q_2$ may split into a pair of planes and, in addition to $K(3,3)$, we obtain the 3-prism graph (see Figure 1 below). Even though this intersection looks degenerate, the two families have the same codimension 5 in the space of all smooth sextic $K3$-surfaces.

The following theorem is the principal result of this paper.

Theorem 1.2 (see §2.4)**.** *The maximal number* `max #` *of split hyperplane sections on a smooth $2d$-polarized $K3$-surface is given by the following table*

$h^2 = 2d$	2	4	6	8	10	12	14	16	18	20	22	24	28
graphs	1	1	2	3	6	9	8	8	5	3	1	1	1
max #	72	72	76	80	16	90	12	24	3	4	1	1	1
h-configs	?	?	9235	860	171	44	21	12	6	3	1	1	1

We list also the number `graphs` *of combinatorial types of h-fragments and, whenever known, the number h-*`configs` *of h-configurations (see Convention 2.10 below).*

Theorem 1.2 is mostly proved by brute force, listing all configurations spanned by h-fragments. (As a result, this gives one a way to answer a number of further questions about the geometry of such configurations.) We outline the principal ideas in §2, upon which, in §3–§8, on a case-by-case basis, we give the necessary details and provide some extra information, such as the structure of the h-fragments, bounds itemized by the types of the fragments, extremal configurations, *etc.* Finally, in §9 we discuss briefly the toy example of hyperelliptic $K3$-surfaces.

1.1. **Acknowledgements.** I am grateful to Igor Dolgachev (who also suggested the original question) and Shigeyuki Kondō for a number of fruitful discussions of this project at its early stages.

2. Split hyperplane sections

In this section, we recall the arithmetical restatement of the problem (see §2.1), classify the h-fragments on birational models (see §2.2), discuss pairwise intersections of h-fragments (see §2.3), and outline the idea of the computation leading to the proof of Theorem 1.2 (see §2.4).

2.1. **Preliminaries** (see [6, 2, 8])**.** Given a graph Γ and an even integer $2d > 0$, we denote

$$\mathcal{F}_{2d}(\Gamma) := (\mathbb{Z}\Gamma + \mathbb{Z}h)/\ker, \quad h^2 = 2d,$$

where, for vertices $u, v \in \Gamma$, we let $u^2 = -2$, $u \cdot h = 1$, and $u \cdot v = 1$ (resp. 0) if u and v are (resp. are not) connected by an edge. More generally, if Γ is a multigraph, $u \cdot v$ is the multiplicity of the edge $[u, v]$. We consider only those graph Γ for which $\mathcal{F}_{2d}(\Gamma)$ is hyperbolic, $\sigma_+\mathcal{F}_{2d}(\Gamma) = 1$. This implies that Γ is either

- *elliptic*, $\sigma_+ = \sigma_0 = 0$ (a union of elliptic Dynkin diagrams), or
- *parabolic*, $\sigma_+ = 0$, $\sigma_0 > 0$ (a union of Dynkin diagrams, elliptic or affine, of which at least one is affine), or
- *hyperbolic*, $\sigma_+ = 1$ (we make no assumption about σ_0).

In the latter case, the property that $\sigma_+\mathcal{F}_{2d}(\Gamma) = 1$ depends on the degree $2d$, *cf.* the *intrinsic polarization* in [2].

Conversely, given a $2d$-polarized hyperbolic lattice $N \ni h$, its *Fano graph* is

$$\operatorname{Fn}(N, h) := \{u \in N \mid u^2 = -2,\ u \cdot h = 1\},$$

where two vertices $u, v \in \operatorname{Fn}(N, h)$ are connected by an edge of multiplicity $u \cdot v$. If $N = NS(X)$ for a smooth $2d$-polarized $K3$-surface $X \subset \mathbb{P}^{d+1}$ and $h \in N$ is the class of hyperplane section, then, by the Riemann–Roch theorem, $\operatorname{Fn}(N, h) = \operatorname{Fn} X$ is indeed the graph of lines on X.

A $2d$-polarized hyperbolic lattice $N \ni h$ is called *m-admissible*, $m = 1, 2, 3$, if there is no vector $e \in N$ such that either

- $e^2 = -2$ and $e \cdot h = 0$ (*exceptional divisor*) or
- $e^2 = 0$ and $e \cdot h = r$ (*r-isotropic vector*), $|r| \leqslant m$.

An m-admissible lattice is called m-geometric if it admits a primitive isometry to the *$K3$-lattice* $\mathbf{L} := 2\mathbf{E}_8 \oplus 3\mathbf{U}$. It is called *$m$-subgeometric* if it has an m-geometric (in particular, m-admissible) finite index extension. Recall, see [13], that finite index extensions $\tilde{N} \supset N$ are in a bijection with isotropic subgroups $\mathcal{K} := \tilde{N}/N \subset \operatorname{discr} N$; those corresponding to m-geometric extensions are called *m-geometric kernels* of N.

Remark 2.1. The 1-admissibility of $N \ni h$ suffices to assert that $u \cdot v \geqslant 0$ for any pair of vertices $u, v \in \operatorname{Fn}(N, h)$, see [8]. If $2d \geqslant 4$ and $N \ni h$ is 2-admissible, one also has $u \cdot v \leqslant 1$ for any pair of vertices, so that $\operatorname{Fn}(N, h)$ is a simple graph.

With the degree $2d$ fixed, a graph Γ is called m-admissible/m-subgeometric if so is the lattice $\mathcal{F}_{2d}(\Gamma) \ni h$. Both properties are hereditary. If Γ is m-admissible, we can speak about the *saturations*

$$\operatorname{sat}\Gamma := \operatorname{Fn}\mathcal{F}_{2d}(\Gamma), \qquad \operatorname{sat}(\Gamma, \mathcal{K}) := \operatorname{Fn}\mathcal{F}_{2d}(\Gamma, \mathcal{K}),$$

where $\mathcal{K}$ is an m-geometric kernel of $\mathcal{F}_{2d}(\Gamma)$ and $\mathcal{F}_{2d}(\Gamma, \mathcal{K})$ is the corresponding finite index extension. An m-subgeometric graph Γ is m-geometric if $\Gamma = \operatorname{sat}(\Gamma, \mathcal{K})$ for an appropriate m-geometric kernel $\mathcal{K}$. Our proof of Theorem 1.2 is based on the following statement, which is an immediate consequence of the general theory of $K3$-surfaces (the global Torelli theorem [14], surjectivity of the period map [12], description of projective models [17], fine moduli space [1], *etc.*)

Theorem 2.2 (*cf.* [6, 2, 8])**.** *A graph Γ is isomorphic to the Fano graph of a smooth $2d$-polarized $K3$-surface $X \subset \mathbb{P}^{d+1}$, $2d \geqslant 4$, if and only if Γ is 2-geometric.* ◁

In the rest of the paper, the parameter m is usually understood (typically $m = 2$ as in Theorem 2.2) or not important (provided that it is consistent throughout a statement) and we often omit it from the terminology.

Remark 2.3. In this paper, graphs represent lines on surfaces and, at the same time, their vertices span Néron–Severi lattices. For this reason, we freely mix graph theoretic, geometric, and arithmetic terminology. Thus, for two vertices $u, v \in \Gamma$, the terms "are adjacent", "intersect", and "$u \cdot v = 1$" are synonyms, and so are the terms "are disjoint/skew" and "$u \cdot v = 0$." Vertices are often referred to as lines.

2.2. **Classification of h-fragments.** Let $X \subset \mathbb{P}^{d+1}$ be a smooth $2d$-polarized $K3$-surface. By definition, an induced subgraph $\Sigma \subset \operatorname{Fn} X$ represents a split hyperplane section (from now on, an *h-fragment*) if $h = \sum_{v \in \Sigma} v$ in $NS(X)$. Using Theorem 2.2, we conclude that an abstract graph Σ can serve as an h-fragment in degree $2d$ if and only if

$$|\Sigma| = 2d, \qquad \Sigma \text{ is 3-regular}, \qquad \Sigma \text{ is 2-subgeometric}. \tag{2.4}$$

Indeed, the last condition means that Σ does appear in the Fano graph of a $K3$-surface, whereas the former two imply that the vector $u := h - \sum_{v\in\Sigma} v$ lies in the radical of the hyperbolic lattice $\mathbb{Z}\Sigma + \mathbb{Z}h$; it follows that u must vanish in $N/\ker N$ any hyperbolic overlattice $N \supset (\mathbb{Z}\Sigma + \mathbb{Z}h)$.

A *bouquet* of h-fragments (at a line $\ell \in \operatorname{Fn} X$) is a union of h-fragments containing ℓ. The *multiplicity* $\operatorname{mult}\ell$ is the number of h-fragments in the maximal bouquet at ℓ, *i.e.*, the total number of h-fragments $\Sigma \subset \operatorname{Fn} X$ containing ℓ. The number of h-fragments in $\operatorname{Fn} X$ is denoted by $\#_\Sigma(X)$.

Remark 2.5. The argument above shows also that the property of Σ to be an h-fragment does not depend on its embedding to $\operatorname{Fn} X$: whenever $\operatorname{Fn} X$ contains an induced subgraph isomorphic to Σ, it represents a split hyperplane section.

Furthermore, whenever $\operatorname{Fn} X$ contains $\Sigma \smallsetminus v$, $v \in \Sigma$, it also contains the missing vertex v, constituting, together with $\Sigma \smallsetminus v$, an h-fragment.

A 3-regular graph cannot be elliptic or parabolic, and we employ the taxonomy of hyperbolic graphs developed in [2, 8]. Order affine Dynkin diagrams according to their Milnor number, followed by $\mathbf{A}_\mu < \mathbf{D}_\mu < \mathbf{E}_\mu$. A hyperbolic graph Γ contains an affine Dynkin diagram as an induce subgraph; we fix a minimal one $\Phi \subset \Gamma$ and call Γ a Φ-graph. This choice splits Γ into two subgraphs

$$\Pi := \Phi \cup \bigl\{ v \in \Gamma \bigm| v \cdot \Phi = 0 \bigr\}, \qquad \sec\Phi := \Gamma \smallsetminus \Pi.$$

The connected components of the parabolic subgraph Π are called *fibers*, whereas the vertices of $\sec\Phi$ are called *sections*. (This terminology is motivated by elliptic pencils on $K3$-surfaces, see [2, 8] for details.) The admissibility assumption imposes certain restrictions, *e.g.*,

$$s \cdot \kappa_\Phi = s \cdot \kappa_{\Phi'} \geqslant s \cdot \Phi''$$

for any section s, parabolic fiber Φ', and elliptic fiber Φ''. (Here, κ_Φ stands for the fundamental cycle of the affine Dynkin diagram Φ; we have $s \cdot \kappa_\Phi = 1$ if s is a simple section.) The assumption that Φ is minimal imposes further restrictions on the number of sections and their pairwise intersections, *cf.* [2, Fig. 1]. Finally, the 3-regularity of Γ leaves us with but the following types of fibers

- parabolic $\tilde{\mathbf{A}}_n$ and elliptic $\mathbf{A}_\mu$, $\mu < n$, if $\Phi \cong \tilde{\mathbf{A}}_n$, $n = 2, 3, 4, 5$, or
- parabolic $\tilde{\mathbf{D}}_5$, $\tilde{\mathbf{A}}_7$ and elliptic $\mathbf{D}_4$, $\mathbf{A}_\mu$, $\mu < 7$, if $\Phi \cong \tilde{\mathbf{D}}_5$,

asserts that there are at most three parabolic fibers, and dictates a precise set $\sec\Phi$ of sections, *viz.* the one that makes all vertices of Φ trivalent. (For the moment, we assume all sections simple.) More precisely, if $\Phi = \{a_1, \ldots, a_{n+1}\} \cong \tilde{\mathbf{A}}_n$, there is a unique section s_i intersecting a_i and disjoint from a_j, $j \neq i$; it is this numbering of the sections that is used in Convention 2.6 below. If $\Phi = \{a_1, \ldots, a_4, b_1, b_2\} \cong \mathbf{D}_5$, there are two sections s_{2i-1}, s_{2i} intersecting each of the monovalent vertices a_i and disjoint from all other vertices.

It remains to run the algorithm of [2, 8] and list all graphs. Note that, since we consider smooth surfaces, [8, Warning 3.6] does not apply: we can freely rule out all intermediate graphs containing an affine Dynkin diagram $\Phi' < \Phi$. We use `GAP` [11] and, most notably, its `digraph` package. The results of this computation are listed in the subsequent sections, separately for each degree.

Convention 2.6. Most graphs found do not have "standard names", and we use an encoding arising from our classification. Namely, we represent a graph as

$$\Phi_1(\mathrm{sec}_1)\,\Phi_2(\mathrm{sec}_2)\,\ldots\,\langle\text{intersections}\rangle.$$

Here, $\Phi_1 := \Phi, \Phi_2, \ldots$ are the fibers; their monovalent vertices are numbered in a certain standard way. Sections are also numbered, and $\mathrm{sec}_i = \mathrm{sec}_{i1}; \mathrm{sec}_{i2}; \ldots$, with sec_{ij} listing the sections intersecting vertex $a_{ij} \in \Phi_i$. The optional part

$$\langle\text{intersections}\rangle = (n_1 \times n_2)(n_3 \times n_4)\ldots$$

lists all pairwise intersections of the sections: *e.g.*, $s_1 \cdot s_2 = 1$ if and only if (1×2) is present on this list.

Within each section, we number the h-fragments Σ_n according to the list found at the beginning of this section. In the tables where the graphs are listed, the first column "Σ" refers to the list and the second one is "(r, g, s)", where

- $r := \operatorname{rk} \mathbb{Z}\Sigma = \operatorname{rk} \mathcal{F}_{2d}(\Sigma)$ or, equivalently, the codimension of the respective stratum in the space of all smooth $2d$-polarized $K3$-surfaces,
- the girth $g := \operatorname{girth} \Sigma$, and
- the size $s := |\operatorname{Aut} \Sigma|$ of the automorphism group (computed by `digraph`).

The other columns are degree specific and explained in the respective sections.

It remains to consider graphs with multisections, *i.e.*, sections s with $s \cdot \kappa_\Phi > 1$. This manual argument is also a good example of the algorithm used above. By [2], Φ must be $\tilde{\mathbf{A}}_2$ or $\tilde{\mathbf{A}}_3$ (or $\tilde{\mathbf{D}}_4$, but the latter has more than trivalent vertices).

If $\Phi = \{a_1, a_2, a_3\} \cong \tilde{\mathbf{A}}_2$, a multisection may (and does, see Remark 2.5) exist only if $2d = 4$, see [2, Lemma 8.3]. This section is necessarily triple, adjacent to all three vertices of Φ, and we obtain the h-fragment $K(4)$.

If $\Phi = \{a_1, a_2, a_3, a_4\} \cong \tilde{\mathbf{A}}_3$, a bisection s_{13} may exist only if $2d = 4$, 6, or 8, see [2, Lemma 7.4]. If $2d = 4$, the graph would have too many (at least 5) vertices. If $2d = 6$, there also is another bisection s_{24} with $s_{13} \cdot s_{24} = 1$, see [2, Lemma 7.6] or Remark 2.5, and we obtain the h-fragment $K(3, 3)$.

Finally, if $2d = 8$, then s_{13} is the only bisection, which is disjoint from all other sections, *cf.* [2, § 5.3]. By the 3-regularity, there should be two other sections s_2, s_4 intersecting a_2, a_4, respectively. Since we need $|\Gamma| = 8$, this leaves but a single extra fiber $\{a_1'\} \cong \mathbf{A}_1$, and we must have $s_{13} \cdot a_1' = s_2 \cdot a_1' = s_4 \cdot a_1' = 1$. By the 3-regularity again, we conclude that $s_2 \cdot s_4 = 1$, so that $\{a_1', s_2, s_4\} \cong \tilde{\mathbf{A}}_2$ and Γ is an $\tilde{\mathbf{A}}_2$-graph (without multisections): it is graph (1) in §5 and Figure 2.

2.3. **Intersections of h-fragments.** Given a graph Σ, a subgraph $\Delta \subset \Sigma$ is called *perfect* if each vertex $u \in \Sigma \smallsetminus \Delta$ is adjacent to at most one vertex $v \in \Delta$. The *perfect complement* of a perfect subgraph is the set (see §4 or §5 for examples)

$$\Sigma \mathbin{\smallsetminus\!\!\smallsetminus} \Delta := \bigl\{u \in \Sigma \smallsetminus \Delta \bigm| u \text{ is not adjacent to any } v \in \Delta\bigr\}.$$

Proposition 2.7. *Let Σ_1, Σ_2 be two h-fragments in an admissible graph Γ. Then:*

1. *the intersection $\Delta := \Sigma_1 \cap \Sigma_2$ is a perfect subgraph of each Σ_i, $i = 1, 2$;*
2. *the relation $(u_1, u_2) \mapsto (u_1 \cdot u_2 = 1)$ on $(\Sigma_1 \smallsetminus \Delta) \times (\Sigma_2 \smallsetminus \Delta)$ is a bijection $\varsigma\colon \Sigma_1 \mathbin{\smallsetminus\!\!\smallsetminus} \Delta \simeq \Sigma_2 \mathbin{\smallsetminus\!\!\smallsetminus} \Delta$, henceforth called the* attachment bijection.

Proof. Since each line intersects each hyperplane at one point (or because $u \cdot h = 1$ and $h = \sum_{v \in \Sigma} v$, *cf.* Remark 2.1), we have

(2.8) each vertex $u \in \Gamma \smallsetminus \Sigma$ is adjacent to exactly one vertex $v \in \Sigma$.

If Δ were not perfect in, say, Σ_1, there would be a vertex $u \in \Sigma_1 \smallsetminus \Delta = \Sigma_1 \smallsetminus \Sigma_2$ adjacent to at least two vertices of $\Delta \subset \Sigma_2$, contradicting (2.8).

Similarly, each vertex of $\Sigma_i \smallsetminus \Delta$ must be adjacent to exactly one vertex of Σ_j, $j \neq i$. The vertices in $(\Sigma_i \smallsetminus \Delta) \smallsetminus (\Sigma_i \ggg \Delta)$ are already adjacent to those in $\Delta \subset \Sigma_j$, leaving a bijection between the perfect complement. □

Our proof of Theorem 1.2 consists in listing all "interesting" graphs by adding one h-fragment at a time. Thus, we start with an admissible graph Γ_0 and an h-fragment Σ and construct a new graph $\Gamma := \Gamma_0 \cup \Sigma$, which must also be admissible. For the new lattice $\mathcal{F}_{2d}(\Gamma)$, we need to choose and fix

- the intersection $\Delta := \Gamma_0 \cap \Sigma$ (or, rather, an isomorphism between a pair of induced subgraphs $\Delta_0 \subset \Gamma_0$ and $\Delta_\Sigma \subset \Sigma$) and
- for each vertex $u \in \Sigma \smallsetminus \Delta_\Sigma$, the set $\Gamma_0(u) := \{v \in \Gamma_0 \mid v \cdot u = 1\}$.

Since we need an admissible graph, these choices are quite limited, and it is this fact that makes the computation feasible. First of all, till the very last moment (*viz.* saturating subgeometric graphs to geometric) we can confine ourselves to the graphs Γ_0 that are unions of h-fragments; then, we can apply Proposition 2.7 to each pair Σ, Σ_0, where $\Sigma_0 \subset \Gamma_0$ is an h-fragment. Besides, we have the following "global" analogue of Proposition 2.7, whose proof is straightforward, *cf.* (2.8).

Proposition 2.9. *Let Σ be an h-fragment and assume that the graph $\Gamma := \Gamma_0 \cup \Sigma$ is admissible. Denote $\Delta := \Gamma_0 \cap \Sigma$. Then*:

1. *Δ is a perfect subgraph of Γ_0 (but not necessarily of Σ);*
2. *the relation $(u_1, u_2) \mapsto (u_1 \cdot u_2 = 1)$ on $(\Gamma_0 \smallsetminus \Delta) \times (\Sigma \smallsetminus \Delta)$ is a function $\varsigma\colon \Gamma_0 \ggg \Delta \to \Sigma \smallsetminus \Delta$, henceforth called the* attachment map. ◁

2.4. **Idea of the proof of Theorem 1.2.** As already explained, for degrees $2d \geqslant 6$ we merely list all 2-geometric graphs Γ such that $\mathcal{F}_{2d}(\Gamma)$ is rationally generated by a union of h-fragment. We use a modified version of the algorithm of [2, 8], adding at each step a whole h-fragment rather than a single vertex. We also use a number of enhancements speeding up the algorithm; the noteworthy ones are listed below.

2.4.1. At each step, the data

$$\Gamma_0 \supset \Delta_0 \simeq \Delta_\Sigma \subset \Sigma \quad \text{and} \quad \bigl\{\Gamma_0(u) \bigm| u \in \Sigma \smallsetminus \Delta_\Sigma\bigr\}$$

controlling the output (see §2.3) are limited using Propositions 2.7 and 2.9. In some cases we use additional restrictions that are degree/graph specific, *cf.*, for example, Lemmata 4.3 and 5.5 below.

2.4.2. Each intermediate graph Γ obtained is replaced with its *h-part*

$$\operatorname{hp}\Gamma := \bigcup \Sigma, \quad \Sigma \subset \operatorname{sat}\Gamma \text{ is an } h\text{-fragment}$$

generating the same lattice over $\mathbb{Q}$; this makes Proposition 2.7 more efficient.

2.4.3. After each step (and upon the normalization as in §2.4.2), multiple copies of the same graph are removed using the `digrap` package.

2.4.4. At each step we insist that the rank $\operatorname{rk}\mathcal{F}_{2d}(\Gamma)$ must increase, as otherwise the new graph would be found among the saturations of the old one.

2.4.5. For configurations of large rank $\operatorname{rk}\mathcal{F}_{2d}(\Gamma) \geqslant r_{\min}$ (a threshold depending on the degree, typically $r_{\min} = 18$), we switch to adding one vertex at a time, literally as in [2, 8]. In this case, §2.4.2 no longer applies.

2.4.6. We also use a few tricks to control the order in which h-fragments are added. For example, typically h-fragments are added in the order $\Sigma_1, \Sigma_2, \ldots$ in which they appear on the lists. A few other degree specific details are discussed in the relevant sections below.

2.4.7. At the end, for further analysis, we compute all geometric graphs containing at least a certain number $\#_{\min}$ of h-fragments. This threshold

$$\begin{array}{rccccc} h^2 = 2d\colon & 6 & 8 & 10 & 12 & \geqslant 14 \\ \#_{\min}\colon & 16 & 9 & 3 & 2 & 1 \end{array}$$

is chosen to keep the computation feasible and avoid large output.

With this said, we consider Theorem 1.2 proved for all degrees $2d \geqslant 6$. □

Convention 2.10. When stating our results, depending on the output obtained, we distinguish between *configurations* (of lines) and *h-configurations*.

A *configuration* is merely a geometric graph; it is called *maximal* if it is not a proper induced subgraph of another configuration.

An h-configuration is a subgeometric graph Ξ with the following properties:

- Ξ is a union (not necessarily disjoint) of h-fragments, and
- there is a geometric graph $\Gamma \supset \Xi$ such that $\Xi = \operatorname{hp}\Gamma$.

It is *maximal* if it is not a proper induced subgraph of another h-configurations.

For example, the algorithm discussed in this section is mostly designed to produce h-configurations. The counts stated in Theorem 1.2 are those of h-configurations, not configurations.

3. Quartics ($h^2 = 4$)

There is a unique h-fragment of degree 4, which is

(1) the complete graph $K(4)$.

Obviously, $\operatorname{rk}\mathbb{Z}\Sigma_1 = 4$, $\operatorname{girth}\Sigma_1 = 3$, and $\operatorname{Aut}\Sigma_1 = \mathbb{S}_4$. Our principal result in this section is the following theorem.

Theorem 3.1. *The number of h-fragments on a smooth quartic $X \subset \mathbb{P}^3$ is*

- 72*, if X is Schur's quartic X_{64}, see* [18, 6];
- 60*, if X has* 60 *lines,* i.e.*, is X'_{60}, X''_{60}, or $\bar{X}''_{60}$ in* [6];
- *less than* 60 *otherwise.*

Remark 3.2. We know a single example of a quartic with 50 h-fragments, *viz.* Y_{56} in [6]; in all other known cases, the number of h-fragments is at most 48. Observe that Y_{56} is also an example of a *real* quartic with 50 *real* h-sections.

Conjecture 3.3. With the exception of the four surfaces mentioned in Theorem 3.1 and Remark 3.2, a smooth quartic $X \subset \mathbb{P}^3$ has at most 48 h-fragments.

Proof of Theorem 3.1. All quartics X with $|\operatorname{Fn} X| > 48$ are known, see [9]; we check the 26 graphs one-by-one and find 72, 60 (as in Theorem 3.1), 50 (as in Remark 3.2), or at most 48 h-fragments. Therefore, henceforth we assume that $|\operatorname{Fn} X| \leqslant 48$.

As is well known (see, *e.g.*, [6]), the star of a line ℓ in the Fano graph of a smooth quartic surface $X \subset \mathbb{P}^3$ is of the form $p\tilde{\mathbf{A}}_2 \oplus q\mathbf{A}_1$, where the values of (p, q) are as in the following table:

$$\begin{array}{rccccccc} p = & 0 & 1 & 2 & 3 & 4 & 5 & 6 \\ q \leqslant & 12 & 10 & 9 & 7 & 6 & 3 & 2 \end{array}$$

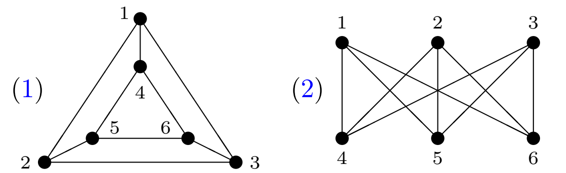

FIGURE 1. The h-fragments of degree 6

TABLE 1. h-configurations of degree 6 (see Convention 4.1)

Σ	(r,g,s)	h-fragment counts	large counts				
(1)	$(6,3,12)$	$0..6, 8..10, 12, 15, 16, 18, 20, 25, 36$	16	·	36	25	36
(2)	$(6,4,72)$	$0..24, 26, 27, 29, 30, 36, 40$	20	36	12	24	40
total counts:		$0..34, 36, 48, 49, 76$	36	36	48	49	76
configuration:			34	36	36	Ψ_{38}	Ψ_{42}

It follows that $\operatorname{mult}\ell \leqslant 6$ for each $\ell \in \operatorname{Fn} X$ and we can easily bound $\#_\Sigma(X)$ by 72: since each h-fragment consists of 4 lines, we have

$$\#_\Sigma(X) \leqslant \frac{\max(\operatorname{mult}\ell)}{4}|\operatorname{Fn} X| \leqslant \frac{6}{4}\cdot 48 = 72. \tag{3.4}$$

To improve this bound, we follow [6] and compute all configurations with a bouquet of six h-fragments, finding no new surface X with $\#_\Sigma(X) > 48$. Hence, we can assume $\max(\operatorname{mult}\ell) \leqslant 5$ in (3.4), arriving at $\#_\Sigma(X) \leqslant 60$.

Finally, under the assumptions, for $\#_\Sigma(X) = 60$ we must have $|\operatorname{Fn} X| = 48$ and $\operatorname{mult}\ell = 5$, hence $\operatorname{val}\ell \geqslant 15$, for *each* line ℓ. Then, mimicking the proof of Segre's theorem [19] cited in the first paragraph of §1, we arrive at $|\operatorname{Fn} X| \geqslant 52$. □

4. SEXTICS ($h^2 = 6$)

A smooth $K3$-sextic $X \subset \mathbb{P}^4$ is a regular complete intersection of a quadric and a cubic, $X = Q_2 \cap Q_3$. There are two h-fragments of degree 6, *viz.*

(1) $\tilde{\mathbf{A}}_2(1;2;3)\ (1\times 2)(1\times 3)(2\times 3)$ (the 3-prism) and
(2) the complete bipartite graph $K(3,3)$ (the utility graph),

see also Figure 1 and Table 1. Geometrically (see §1), cutting $X = Q_2 \cap Q_3$ by a hyperplane H, the two split sections differ by whether $H \cap Q_2$ is a smooth quadric $\mathbb{P}^1 \times \mathbb{P}^1$ or a pair of planes $\mathbb{P}^2 \cup \mathbb{P}^2$.

Convention 4.1. Listed in Tables 1, 2, 3, are the values taken by the number of h-fragments, both total and itemized by the type of the graphs, and, in the last column, the itemized counts for a few largest h-configurations. In the last row, for each of these few largest h-configurations, we show the corresponding (minimal) configuration, either by its "name" in [2, 7, 8] or just by the number of lines.

As in the case of quartics (see Theorem 3.1), the two largest configurations Ψ_{38}, Ψ_{42} maximize also the number of lines, see [2]; they are triangular (or $\tilde{\mathbf{A}}_2$-, see §2.2). The other three are quadrangular (or $\tilde{\mathbf{A}}_3$-, see §2.2); they can be identified by the triples $(|\Gamma|, \operatorname{rk}\mathbb{Z}\Gamma, |\operatorname{Aut}\Gamma|)$, which are as follows:

$$(16+20) \mapsto (34, 18, 32), \quad (0+36) \mapsto (36, 19, 24), \quad (36+12) \mapsto (36, 18, 1296).$$

Probably, they will be given "names" in [10].

Our original strategy for proving the bound $\#_\Sigma(X) \leqslant 76$ was bounding the multiplicities $\operatorname{mult}\ell$ first and then arguing as in §3. We found that this requires almost as much computation as compiling the full list of h-configurations. Nevertheless, we discuss a few simple facts concerning bouquets of h-fragments of degree 6.

Ultimately, denoting by c_i the number of copies of Σ_i, we have

$$\begin{array}{rccccccccccc} c_2 = & 0 & 1 & 2 & 3 & 4 & 5 & 6 & 7 & 8 & 9 & 10 \\ c_1 \leqslant & 5 & 6 & 6 & 5 & 5 & 6 & 6 & 4 & 5 & 0 & 0 \end{array}$$

If $c_2 = 8$, then $c_1 \in \{0, 2, 5\}$. To describe the structure of a bouquet, recall (see [2, § 2.5]) that the star of a vertex $\ell \in \operatorname{Fn} X$ is of the form

$$p\mathbf{A}_2 \oplus q\mathbf{A}_1, \qquad p \leqslant 1, \quad q \leqslant 9, \quad q \neq 8 \text{ if } p = 1. \tag{4.2}$$

By Proposition 2.7, two h-fragments intersects in a perfect subset Δ. Up to automorphism, proper perfect subsets are: in Σ_1,

(1) $\Delta = \{1\}$, with $\Sigma_1 \smallsetminus \Delta = \{5, 6\}$;
(2) $\Delta = \{1, 4\}$, with $\Sigma_1 \smallsetminus \Delta = \varnothing$;
(3) $\Delta = \{1, 2, 3\}$, with $\Sigma_1 \smallsetminus \Delta = \varnothing$,

and in Σ_2,

(4) $\Delta = \{1\}$, with $\Sigma_2 \smallsetminus \Delta = \{2, 3\}$;
(5) $\Delta = \{1, 4\}$, with $\Sigma_2 \smallsetminus \Delta = \varnothing$.

Here and below, we index the vertices $v_k \in \Sigma_i$ as shown in the figures, and we often abbreviate v_k to just k.

The following lemma can be used to speed up the computation, see §2.4.1.

Lemma 4.3. *The intersection $\Delta := \Sigma_1 \cap \Sigma_1'$ of two copies of Σ_1 is either empty or a common triangle.*

Proof. If Σ_1 contains a line ℓ, it must also contain an $\mathbf{A}_2$-subgraph in the star of ℓ. According to (4.2), this subgraph is unique. □

We arive at the following description of a bouquet. Let S be the set of the $\mathbf{A}_1$-components of the star of ℓ; we have $|S| \leqslant 9$, see (4.2). Replacing each h-fragment $\Sigma \ni \ell$ with its *germ* at ℓ, *i.e.*, the set of its vertices that are adjacent to ℓ, we get a set $\mathfrak{S}_1 \subset S$ (the germs of Σ_1-fragments without the common $\mathbf{A}_2$-type component) and a set $\mathfrak{S}_2$ of 3-element subsets of S (the germs of Σ_2-fragments). The latter has the property that

$$|s' \cap s''| \leqslant 1 \quad \text{for any pair } s', s'' \in \mathfrak{S}_2,\ s' \neq s''.$$

The attachment bijections are less straightforward, and we omit their description.

5. Octics ($h^2 = 8$)

A typical smooth octic $K3$-surface $X \subset \mathbb{P}^5$ is a *triquadric*, *i.e.*, regular complete intersection of three quadric hypersurfaces. However, in the space of all octics there is a divisor of *special* octics which cannot be represented in this way. According to [17] (see also [8] for a homological restatement), a smooth octic X is a triquadric if and only if the polarized lattice $NS(X) \ni h$ is 3-admissible.

There are three h-fragments of degree 8:

(1) $\tilde{\mathbf{A}}_2(1;2;3)\ \mathbf{A}_1(1,2,3)\ \mathbf{A}_1(1,2,3)$;
(2) $\tilde{\mathbf{A}}_3(1;2;3;4)\ (1 \times 2)(1 \times 3)(2 \times 4)(3 \times 4)$ (the Wagner graph);

(1) (2) (3)

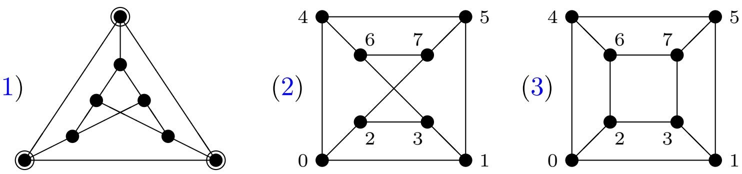

FIGURE 2. The h-fragments of degree 8

TABLE 2. h-configurations of degree 8 (see Convention 4.1)

Σ	(r, g, s)	h-fragment counts	large counts						
(1)	$(8, 3, 12)$	$0..10, 12, 14, 16, 18, 20, 36, 42, 72$	72						
(2)	$(8, 4, 16)$	$0..16, 18..21, 24, 32, 48$		24	16	48	32	48	$\cdot$
(3)	$(8, 4, 48)$	$0..13, 16, 20, 21, 32, 80$		12	20	8	32	16	80
total (2) + (3):		$0..18, 20, 21, 23, 24, 26, 36, 56, 64, 80$		36	36	56	64	64	80
configuration:			Ψ_{33}	28	28	Θ'_{32}	Θ''_{32}	Θ'''_{32}	Θ^{K}_{32}

(3) $\tilde{\mathbf{A}}_3(1; 2; 3; 4)$ $(1 \times 2)(1 \times 4)(2 \times 3)(3 \times 4)$ (the 3-cube),

see also Figure 2 and Table 2 (where Σ_1 and Σ_2, Σ_3 are treated separately due to Proposition 5.1 below).

The maximal number 72 of Σ_1-type fragments is attained at the configuration Ψ_{33} maximizing the number of lines on *special* octics, see [2, Theorem 1.3]. Unlike the cases of quartics and sextics, the Kummer triquadric Θ^{K}_{32} with the maximal number of h-fragments is not line maximizing (and all its fragments are of the same type). One of the two line-maximizing configurations, *viz.* $\Theta'_{36} \supset \Theta'_{34} \supset \Theta'_{32}$, has but 56 h-fragments; the other one, Θ''_{36}, has no h-fragments at all.

Proposition 5.1. *The fragment Σ_1 appears in special octics only, whereas Σ_2, Σ_3 appear in triquadrics only.*

Proof. The fragment Σ_1 has a 3-isotropic vector, *e.g.*, the sum of the three vertices (circled in Figure 2) of the outer triangle. For $\Sigma = \Sigma_2$ or Σ_3, we try to append a 3-isotropic vector p, *i.e.*, consider the lattice

$$\mathcal{N} := (\mathbb{Z}\Sigma + \mathbb{Z}h + \mathbb{Z}p)/\ker, \qquad p^2 = 0, \quad p \cdot h = 3.$$

This notation is ambiguous as we do not know the intersections of p with the vertices of Σ. By [8, Lemma 2.29], and since $h = \sum_{v \in \Sigma} v$, there is a 3-element subset $o \subset \Sigma$ such that $p \cdot v = 1$ if $v \in o$ and $p \cdot v = 0$ otherwise. We try all such subsets and find that the polarized lattice $\mathcal{N} \ni h$ is not 2-admissible.

There are five $\operatorname{Aut} \Sigma_2$-orbits of 3-element subsets $o \subset \Sigma_2$:

- $o = \{0, 1, 2\}$ or $\{0, 2, 4\}$: the lattice is not hyperbolic, $\sigma_+\mathcal{N} = 2$;
- $o = \{0, 1, 6\}$: there is an exceptional divisor $v_2 + v_3 + v_7 - p$;
- $o = \{0, 2, 5\}$: there is an exceptional divisor $v_3 + v_4 + v_6 - p$;
- $o = \{0, 3, 5\}$: there is an exceptional divisor $v_4 + v_6 + v_7 - p$,

and three $\operatorname{Aut} \Sigma_3$-orbits of 3-element subsets $o \subset \Sigma_3$:

- $o = \{0, 1, 2\}$: the lattice is not hyperbolic, $\sigma_+\mathcal{N} = 2$;
- $o = \{0, 1, 6\}$: there is an exceptional divisor $v_2 + v_3 + v_7 - p$;
- $o = \{0, 3, 5\}$: there is an exceptional divisor $v_4 + v_6 + v_7 - p$.

This concludes the proof. □

Remark 5.2. In the proof, the exceptional divisor is of the form $-p + \sum_{v\in\Xi} v$, where $\Xi \subset \Sigma$ is an induced subgraph isomorphic to $\mathbf{A}_3$ and disjoint from o. Such a divisor exists for any 3-element set $o \subset \Sigma$; it can be used instead of $\sigma_+\mathcal{N}$.

Remark 5.3. According to [2, § 2.5], one has $\operatorname{val}\ell \leqslant 7$ for each vertex ℓ of the Fano graph $\operatorname{Fn} X$ of a smooth triquadric X, and configurations with 7-valent vertices do appear on our list of configurations, *e.g.*, $\Theta'_{36} \supset \Theta'_{34}$. Nevertheless, experimentally we observe that $\operatorname{val}\ell \leqslant 6$ *in the h-part* $\operatorname{hp}(\operatorname{Fn} X)$. Alternatively, this fact could be proved by considering the few dozens of minimal bouquets whose h-fragments together make use of all seven vertices adjacent to ℓ, *cf.* the discussion of bouquets below. We omit this routine search for exceptional divisors.

Problem 5.4. Geometrically, Σ_2 and Σ_3 represent split degree 8 curves serving as base loci of certain nets of quadrics in $\mathbb{P}^4$. It appears that Σ_3 is generic whereas Σ_2 is degenerate, even though they have the same codimension, but we do not know a precise explanation of this phenomenon.

The number of isomorphism classes of bouquets (837) is almost the same as that of configurations (860). It appears that only bouquets of Σ_3-fragments have a nice description. The proper perfect subsets of Σ_3 are, up to automorphism,

(1) $\Delta = \{0\}$, with $\Sigma_3 \smallsetminus \Delta = \{3, 5, 6, 7\}$;
(2) $\Delta = \{0, 2\}$, with $\Sigma_3 \smallsetminus \Delta = \{5, 7\}$;
(3) $\Delta = \{0, 7\}$, with $\Sigma_3 \smallsetminus \Delta = \varnothing$;
(4) $\Delta = \{0, 1, 2, 3\}$, with $\Sigma_3 \smallsetminus \Delta = \varnothing$,

and we can assume that v_0 in each fragment is the central line of the bouquet.

The following lemma speeds up the computation, see §2.4.1.

Lemma 5.5. *There are the following extra restrictions on* $\Delta := \Sigma_3 \cap \Sigma'_3$:

- $|\Delta| \neq 1$, i.e., *case (1) is not realizable*;
- *in case (2), the attachment bijection* $\Sigma_3 \smallsetminus \Delta \to \Sigma'_3 \smallsetminus \Delta$ *is* $(5, 7) \leftrightarrow (7', 5')$.

Proof. In case (1), up to automorphisms of the two graphs, the attachment bijection is either $\varsigma\colon (3, 5, 6, 7) \leftrightarrow (3', 5', 6', 7')$ or $(3, 5, 6, 7) \leftrightarrow (3', 5', 7', 6')$; each results in a number of exceptional divisors, *e.g.*,

$$e = -h + v_4 + v_5 + v_6 + v_7 + v'_4 + v'_5 + v'_6 + v'_7.$$

In case (2), the bijection $\varsigma\colon (5, 7) \leftrightarrow (5', 7')$ results in the exceptional divisor

$$e = -h + 2v_2 + v_3 + v_6 + v_7 + v'_3 + v'_6 + v'_7,$$

leaving $\varsigma\colon (5, 7) \leftrightarrow (7', 5')$ as the only choice. □

Hence, we have the following simple description of a bouquet of Σ_3-fragments at a line ℓ. Let S be the set of lines adjacent to ℓ; by Remark 5.3, we can assume $|S| \leqslant 6$. Replacing each Σ_3-fragment with its germ at ℓ, we obtain a set $\mathfrak{S}_3$ of 3-element subsets $s \subset S$, and the rest of the graph is recovered from $\mathfrak{S}_3$ by Lemma 5.5.

There are no immediate restrictions on $\mathfrak{S}_3$, as the set of all 3-element subsets gives rise to a geometric graph. Hence, all other graphs are subgeometric, but not all of them are saturated. Altogether, there are 14 isomorphism classes of saturated pairs (bouquet, ℓ); their numbers of Σ_3-fragments are

$$1, 2, 2, 2, 3, 3, 4, 4, 4, 5, 5, 7, 8, 20.$$

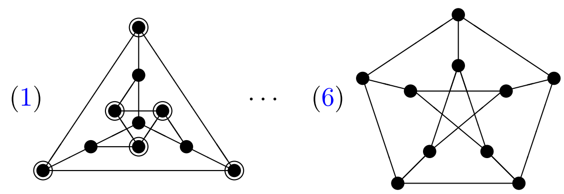

Figure 3. Some h-fragments of degree 10

Table 3. h-configurations of degree 10 (see Convention 4.1)

Σ	(r,g,s)	h-fragment counts	large counts								
(1)	$(9,3,12)$	$0,1,3,6,15$	·	·	·	·	·	·	·	15	·
(2)	$(10,4,4)$	$0..6$	·	·	·	·	·	·	·	·	·
(3)	$(10,4,8)$	$0..6,8$	6	·	·	·	·	·	·	·	·
(4)	$(10,4,20)$	$0..4,6,8,12$	6	12	8	6	6	·	·	·	·
(5)	$(10,4,20)$	$0..4,6,12$	·	·	4	6	6	12	·	·	·
(6)	$(10,5,120)$	$0..8,11,14,16$	·	·	·	·	·	2	14	·	16
total counts:		$0..12,14..16$	12	12	12	12	12	14	14	15	16
configuration:			26	20	20	20	20	20	Φ'''_{30}	22	28

Remark 5.6. The maximal bouquet with 20 copies of Σ_3 is the graph Θ^{K}_{32} that maximizes the number of h-fragments. In this configuration, all 32 bouquets are isomorphic, each consisting of 20 fragments.

Remark 5.7. As a technical detail, in the computation for triquadrics the graphs are processed in the order Σ_3, Σ_2, see §2.4.6.

6. The polarization $h^2 = 10$

There are six h-fragments of degree 10:

(1) $\tilde{\mathbf{A}}_2(1;2;3)$ $\tilde{\mathbf{A}}_2(1;2;3)$ $\mathbf{A}_1(1,2,3)$;
(2) $\tilde{\mathbf{A}}_3(1;2;3;4)$ $\mathbf{A}_2(1,2;3,4)$ $(1\times 3)(2\times 4)$;
(3) $\tilde{\mathbf{A}}_3(1;2;3;4)$ $\mathbf{A}_1(1,2,4)$ $\mathbf{A}_1(2,3,4)$ (1×3);
(4) $\tilde{\mathbf{A}}_3(1;2;3;4)$ $\mathbf{A}_2(1,3;2,4)$ $(1\times 2)(3\times 4)$;
(5) $\tilde{\mathbf{A}}_3(1;2;3;4)$ $\mathbf{A}_2(1,4;2,3)$ $(1\times 2)(3\times 4)$;
(6) $\tilde{\mathbf{A}}_4(1;2;3;4;5)$ $(1\times 3)(1\times 4)(2\times 4)(2\times 5)(3\times 5)$ (Petersen graph),

see also Figure 3 (where only two graphs are shown, merely to illustrate how weird these graphs can be; though, *cf.* also Remark 6.1 below) and Table 3.

Among the three line-maximizing configurations only one, *viz.* Φ'''_{30} (see [2]) has many h-fragments, *viz.* 14 copies of the Petersen graph Σ_6. The other two have no h-fragments at all.

Remark 6.1. This is the first degree where the strata of surfaces with a fixed h-fragment Σ_i may have different codimension $r := \operatorname{rk}\Sigma_i$. In a sense, Σ_1 is "less degenerate" than the others. Geometrically, this hyperplane section contains two parabolic fibers of the same elliptic pencil, *viz.* the two triangles with circled vertices in Figure 3, left. It is worth mentioning that this special graph Σ_1 never appears together with any other h-fragment in the same configuration.

TABLE 4. h-configurations of degree 12 (see Convention 7.1)

Σ	(r,g,s)	h-fragment counts																											
(1)	$(10,3,36)$	20	4	1	·	·	·	·	·	·	·	·	·	·	·	·	·	·	·	·	·	·	·	·	·	·	·	·	·
(2)	$(10,4,24)$	·	·	·	1	·	·	·	·	·	·	·	·	·	·	·	·	·	·	·	·	·	·	·	·	·	·	·	·
(3)	$(10,4,24)$	·	·	·	·	1	·	·	·	·	·	·	·	·	·	·	·	·	·	·	·	·	·	·	·	·	·	·	·
(4)	$(11,4,16)$	·	·	·	·	·	3	1	·	·	·	·	·	·	·	·	·	·	·	·	·	·	·	·	·	·	·	·	·
(5)	$(12,4,4)$	·	·	·	·	·	·	·	16	4	3	2	1	1	·	·	·	·	·	·	·	·	·	·	·	·	·	·	·
(6)	$(12,4,8)$	·	·	·	·	·	·	·	·	·	·	·	1	·	6	1	·	·	·	·	·	·	·	·	·	·	·	·	·
(7)	$(12,4,48)$	·	·	·	·	·	·	·	·	·	·	·	·	·	·	·	16	2	1	·	·	·	·	·	·	·	·	·	·
(8)	$(12,5,16)$	·	·	·	·	·	·	·	·	·	·	·	·	·	·	·	·	·	·	90	10	6	4	3	2	1	·	·	·
(9)	$(12,5,18)$	·	·	·	·	·	·	·	·	·	·	·	·	·	·	·	·	·	·	·	·	·	·	·	·	·	3	2	1
	h-configs:									2		6						2					3	3	5			2	

Remark 6.2. As a technical detail (see §2.4.6), when the first copy of Σ_6 is added to a graph Γ_0 containing $\Sigma_1, \ldots, \Sigma_5$ only, *and if* $\Delta := \Sigma_6 \cap \Gamma_0$ *is to be empty*, we proceed in two steps: first, a pentagon $\tilde{\mathbf{A}}_4$ is added, and then the rest of Σ_6. For some graphs Γ_0 this trick speeds up the computation.

7. THE POLARIZATION $h^2 = 12$

There are nine h fragments of degree 12:

(1) $\tilde{\mathbf{A}}_2(1;2;3)$ $\tilde{\mathbf{A}}_2(1;2;3)$ $\tilde{\mathbf{A}}_2(1;2;3)$;
(2) $\tilde{\mathbf{A}}_3(1;2;3;4)$ $\tilde{\mathbf{A}}_3(1;2;3;4)$ $(1\times 2)(3\times 4)$;
(3) $\tilde{\mathbf{A}}_3(1;2;3;4)$ $\tilde{\mathbf{A}}_3(1;2;4;3)$ $(1\times 2)(3\times 4)$;
(4) $\tilde{\mathbf{A}}_3(1;2;3;4)$ $\tilde{\mathbf{A}}_3(1;2;3;4)$ $(1\times 3)(2\times 4)$;
(5) $\tilde{\mathbf{A}}_3(1;2;3;4)$ $\mathbf{A}_2(1,2;3,4)$ $\mathbf{A}_2(1,3;2,4)$;
(6) $\tilde{\mathbf{A}}_3(1;2;3;4)$ $\mathbf{A}_2(1,2;3,4)$ $\mathbf{A}_2(1,4;2,3)$;
(7) $\tilde{\mathbf{A}}_3(1;2;3;4)$ $\mathbf{A}_2(1,3;2,4)$ $\mathbf{A}_2(1,3;2,4)$;
(8) $\tilde{\mathbf{A}}_4(1;2;3;4;5)$ $\mathbf{A}_1(1,4,5)$ $\mathbf{A}_1(2,3,5)$ $(1\times 3)(2\times 4)$;
(9) $\tilde{\mathbf{A}}_4(1;2;3;4;5)$ $\mathbf{A}_1(1,2,5)$ $\mathbf{A}_1(3,4,5)$ $(1\times 3)(2\times 4)$,

see also Table 4. We conclude that $\#_\Sigma(X) \leqslant 90$ is the sharp bound.

Convention 7.1. In Tables 4–7, we show the itemized h-fragment conunts for each h-configuration, listed one-by-one (except Table 4, where h-configurations with the same conuts are combined; their number, if greater than 1, is given in the last row). In Tables 6 and 7, the last row is the number of configurations.

The four largest h-configurations are as follows:

- $90 \times \Sigma_8$ is the only line-maximizing graph Φ''_{36}, see [2]; its automorphism group is transitive, each bouquet consisting of 30 h-fragments;
- $20 \times \Sigma_1$ is a certain maximal triangular configuration Γ with 21 lines, not transitive; one has $\operatorname{rk} \mathbb{Z}\Gamma = 14$ and $|\operatorname{Aut}\Gamma| = 4320$.
- $16 \times \Sigma_7$ is a certain maximal quadrangular configuration Γ with 24 lines; it is transitive, each bouquet consisting of eight h-fragments, and one has $\operatorname{rk} \mathbb{Z}\Gamma = 14$ and $|\operatorname{Aut}\Gamma| = 768$;
- $16 \times \Sigma_5$ is a certain quadrangular configuration Γ with 24 lines, neither transitive nor maximal; one has $\operatorname{rk} \mathbb{Z}\Gamma = 17$ and $|\operatorname{Aut}\Gamma| = 64$.

Table 5. h-configurations of degree 14 (see Convention 7.1)

Σ	(r, g, s)	h-configurations																				
(1)	$(13, 4, 4)$	2	1	·	·	·	·	·	·	·	·	·	·	·	·	·	·	·	·	·	·	·
(2)	$(13, 4, 16)$	1	·	3	1	·	·	·	·	·	·	·	·	·	·	·	·	·	·	·	·	·
(3)	$(14, 5, 4)$	·	·	·	·	8	3	2	2	2	1	·	·	·	·	·	·	·	·	·	·	·
(4)	$(14, 5, 8)$	·	·	·	·	·	·	·	·	·	·	3	2	1	·	·	·	·	·	·	·	·
(5)	$(14, 5, 8)$	·	·	·	·	4	·	2	·	·	·	·	·	·	2	1	·	·	·	·	·	·
(6)	$(14, 5, 12)$	·	·	·	·	·	·	·	·	·	·	·	·	·	·	·	4	2	1	·	·	·
(7)	$(14, 5, 14)$	·	·	·	·	·	·	·	·	·	·	·	·	·	·	·	·	·	·	1	·	·
(8)	$(14, 6, 336)$	·	·	·	·	·	·	·	·	·	·	·	·	·	·	·	·	·	·	·	2	1

Remark 7.2. As a technical detail, we act as in Remark 6.2 when the first copy of Σ_9 is added to a graph Γ_0 and if $\Delta := \Sigma_6 \cap \Gamma_0$ is to be empty.

8. Higher degrees

Starting from degree $h^2 = 14$, we find all *configurations* containing at least one h-fragment, that is, starting the computation with an h-fragment Σ, we immediately switch to adding one vertex at a time, see §2.4.5.

If $2d \geqslant 14$, all h-configurations are geometric.

8.1. **The case $h^2 = 14$.** There are eight h-fragments of degree 14:

(1) $\tilde{\mathbf{A}}_3(1;2;3;4)$ $\tilde{\mathbf{A}}_3(1;2;4;3)$ $\mathbf{A}_2(1,3;2,4)$;
(2) $\tilde{\mathbf{A}}_3(1;2;3;4)$ $\tilde{\mathbf{A}}_3(1;2;3;4)$ $\mathbf{A}_2(1,3;2,4)$;
(3) $\tilde{\mathbf{A}}_4(1;2;3;4;5)$ $\mathbf{A}_3(3,5;2;1,4)$ $\mathbf{A}_1(2,4,5)$ (1×3);
(4) $\tilde{\mathbf{A}}_4(1;2;3;4;5)$ $\mathbf{A}_2(1,4;2,5)$ $\mathbf{A}_2(2,4;3,5)$ (1×3);
(5) $\tilde{\mathbf{A}}_4(1;2;3;4;5)$ $\mathbf{A}_3(3,4;2;1,5)$ $\mathbf{A}_1(2,4,5)$ (1×3);
(6) $\tilde{\mathbf{A}}_4(1;2;3;4;5)$ $\mathbf{A}_2(1,4;2,3)$ $\mathbf{A}_1(1,3,5)$ $\mathbf{A}_1(2,4,5)$;
(7) $\tilde{\mathbf{A}}_4(1;2;3;4;5)$ $\mathbf{A}_2(1,2;3,4)$ $\mathbf{A}_1(1,3,5)$ $\mathbf{A}_1(2,4,5)$;
(8) $\tilde{\mathbf{A}}_5(1;2;3;4;5;6)$ $\mathbf{A}_1(1,3,5)$ $\mathbf{A}_1(2,4,6)$ $(1 \times 4)(2 \times 5)(3 \times 6)$,

see also Table 5. The only configuration with twelve h-fragments (*viz.* eight copies of Σ_3 and four copies of Σ_5) is a maximal $\tilde{\mathbf{D}}_4$-graph with 26 vertices.

8.2. **The case $h^2 = 16$.** There are eight h-fragments of degree 16:

(1) $\tilde{\mathbf{A}}_3(1;2;3;4)$ $\tilde{\mathbf{A}}_3(1;2;3;4)$ $\tilde{\mathbf{A}}_3(1;2;4;3)$;
(2) $\tilde{\mathbf{A}}_3(1;2;3;4)$ $\tilde{\mathbf{A}}_3(1;2;4;3)$ $\tilde{\mathbf{A}}_3(1;3;2;4)$;
(3) $\tilde{\mathbf{A}}_3(1;2;3;4)$ $\tilde{\mathbf{A}}_3(1;2;3;4)$ $\tilde{\mathbf{A}}_3(1;2;3;4)$;
(4) $\tilde{\mathbf{A}}_4(1;2;3;4;5)$ $\tilde{\mathbf{A}}_4(1;2;3;5;4)$ $\mathbf{A}_1(2,4,5)$ (1×3);
(5) $\tilde{\mathbf{A}}_4(1;2;3;4;5)$ $\tilde{\mathbf{A}}_4(1;2;3;4;5)$ $\mathbf{A}_1(2,4,5)$ (1×3);
(6) $\tilde{\mathbf{A}}_4(1;2;3;4;5)$ $\mathbf{A}_3(1,2;4;3,5)$ $\mathbf{A}_3(1,3;4;2,5)$;
(7) $\tilde{\mathbf{A}}_4(1;2;3;4;5)$ $\mathbf{A}_3(1,4;2;3,5)$ $\mathbf{A}_3(1,3;5;2,4)$;
(8) $\tilde{\mathbf{A}}_5(1;2;3;4;5;6)$ $\mathbf{A}_2(1,3;2,6)$ $\mathbf{A}_2(3,5;4,6)$ $(1 \times 4)(2 \times 5)$,

see also Table 6. The configuration with 24 copies of Σ_8 is the only line-maximizing graph Δ'_{32}, see [2]. Each line is contained in twelve h-fragments. The $K3$-surface is singular and Kummer: the 32 lines split into two disjoint 16-tuples of pairwise skew ones, constituting an abstract configuration $(16_4, 16_4)$.

Table 6. h-configurations of degree 16 (see Convention 7.1)

Σ	(r,g,s)	h-configurations											
(1)	$(14,4,8)$	4	1	·	·	·	·	·	·	·	·	·	·
(2)	$(14,4,24)$	·	·	1	·	·	·	·	·	·	·	·	·
(3)	$(14,4,48)$	·	·	·	4	1	·	·	·	·	·	·	·
(4)	$(14,5,12)$	·	·	·	·	·	1	·	·	·	·	·	·
(5)	$(14,5,12)$	·	·	·	·	·	·	1	·	·	·	·	·
(6)	$(16,5,4)$	·	·	·	·	·	·	·	1	·	·	·	·
(7)	$(16,5,6)$	·	·	·	·	·	·	·	·	1	·	·	·
(8)	$(16,6,96)$	·	·	·	·	·	·	·	·	·	24	2	1
configurations:		1	2	5	1	1	2	2	6	4	1	1	7

Table 7. h-configurations of degree 18 and 20 (see Convention 7.1)

Σ	(r,g,s)	h-configurations					
(1)	$(16,5,8)$	1	·	·	·	·	·
(2)	$(16,5,8)$	·	1	·	·	·	·
(3)	$(17,5,4)$	·	·	1	·	·	·
(4)	$(17,6,8)$	·	·	·	1	·	·
(5)	$(17,6,24)$	·	·	·	·	3	1
configurations:		1	1	4	3	1	1

Σ	(r,g,s)	h-configs		
(1)	$(16,6,240)$	1	·	·
(2)	$(17,6,48)$	·	1	·
(3)	$(18,5,20)$	·	·	4
configurations:		1	1	1

8.3. **The case $h^2 = 18$.** There are five h-fragments:

(1) $\tilde{\mathbf{A}}_4(1;2;3;4;5)$ $\tilde{\mathbf{A}}_4(1;4;2;5;3)$ $\mathbf{A}_3(1,2;4;3,5)$;
(2) $\tilde{\mathbf{A}}_4(1;2;3;4;5)$ $\tilde{\mathbf{A}}_4(1;2;5;3;4)$ $\mathbf{A}_3(2,3;5;1,4)$;
(3) $\tilde{\mathbf{A}}_4(1;2;3;4;5)$ $\tilde{\mathbf{A}}_4(1;2;5;3;4)$ $\mathbf{A}_3(1,3;5;2,4)$;
(4) $\tilde{\mathbf{A}}_5(1;2;3;4;5;6)$ $\tilde{\mathbf{A}}_5(1;2;6;4;5;3)$ $(1\times 4)(2\times 5)(3\times 6)$;
(5) $\tilde{\mathbf{A}}_5(1;2;3;4;5;6)$ $\tilde{\mathbf{A}}_5(1;2;3;4;5;6)$ $(1\times 4)(2\times 5)(3\times 6)$,

see also Table 7, left. All h-fragments are geometric, but not necessarily maximal. The configuration with three copies of Σ_5 is a $\tilde{\mathbf{D}}_4$-graph with 24 vertices.

8.4. **The case $h^2 = 20$.** There are three h-fragments:

(1) $\tilde{\mathbf{A}}_5(1;2;3;4;5;6)$ $\tilde{\mathbf{A}}_5(1;2;3;4;5;6)$ $\mathbf{A}_1(1,3,5)$ $\mathbf{A}_1(2,4,6)$;
(2) $\tilde{\mathbf{A}}_5(1;2;3;4;5;6)$ $\tilde{\mathbf{A}}_5(1;3;2;4;6;5)$ $\mathbf{A}_2(2,5;3,6)$ (1×4);
(3) $\tilde{\mathbf{A}}_4(1;2;3;4;5)$ $\tilde{\mathbf{A}}_4(1;2;3;4;5)$ $\tilde{\mathbf{A}}_4(1;4;2;5;3)$,

see also Table 7, right. The graphs Σ_1, Σ_2 are geometric and maximal, and the graph with four copies of Σ_3 is Φ_{25} in [2]: it is one of the three line-maximizing configurations. The other two, Δ'_{25} and Λ_{25}, have no h-fragments.

8.5. **The case $h^2 = 22$.** For each of the remaining values $h^2 = 22$, 24, 28, there is a single h-fragment Σ_1, which is contained in a single configuration, *viz.* Σ_1 itself, which is maximal. For $h^2 = 22$, the graph Σ_1 is encoded as follows:

(1) $\tilde{\mathbf{A}}_5(1;2;3;4;5;6)$ $\tilde{\mathbf{A}}_5(1;4;5;2;6;3)$ $\mathbf{A}_4(3,5;1;2;4,6)$.

One has $\operatorname{rk}\mathbb{Z}\Sigma_1 = 19$, $\operatorname{girth}\Sigma_1 = 6$, and $\operatorname{Aut}\Sigma_1 \simeq \mathbb{D}_8$.

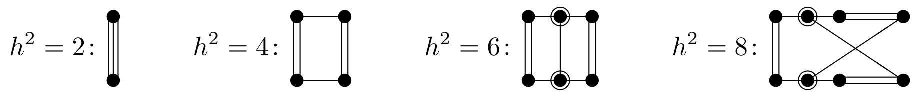

FIGURE 4. Hyperelliptic h-fragments

8.6. **The case $h^2 = 24$.** The only h-fragment Σ_1 in degree 24 is

(1) $\tilde{\mathbf{A}}_5(1;2;3;4;5;6)$ $\tilde{\mathbf{A}}_5(1;2;5;6;3;4)$ $\tilde{\mathbf{A}}_5(1;4;5;2;3;6)$.

One has $\operatorname{rk}\mathbb{Z}\Sigma_1 = 18$, $\operatorname{girth}\Sigma_1 = 6$, and $\operatorname{Aut}\Sigma_1 \simeq \mathbb{S}_4 \times \mathbb{S}_3$. This graph is $\Lambda_{24}^{\mathrm{A}}$, *i.e.*, the only 3-regular graph in [2, Addendum 3.7]. It is one of the several line-maximizing graphs in degree 24.

8.7. **The case $h^2 = 28$.** The only h-fragment Σ_1 in degree 28 is

(1) $\tilde{\mathbf{D}}_5(1,2;3,4;5,6;7,8)$ $\tilde{\mathbf{D}}_5(1,5;3,7;2,8;4,6)$ $\tilde{\mathbf{A}}_7(1;7;6;2;3;5;8;4)$.

One has $\operatorname{rk}\mathbb{Z}\Sigma_1 = 20$, $\operatorname{girth}\Sigma_1 = 7$ (the only h-fragment Σ with $\operatorname{girth}\Sigma > 6$), and $\operatorname{Aut}\Sigma_1 \simeq PSL(3,\mathbb{F}_2) \rtimes (\mathbb{Z}/2)$ is of order 336. This graph is Λ_{28} in [2]. In other words, in degree 28, in the only line-maximizing configuration Λ_{28} all lines lie in a hyperplane. Simple as it is, this fact was not observed before.

9. HYPERELLIPTIC MODELS

As a toy example, we discuss briefly smooth hyperelliptic models of $K3$-surfaces, see [2, § 5.5]. Hyperelliptic h-fragments are no longer simple graphs, and they exist only in degrees $h^2 \leqslant 8$, see Figure 4. We summarize the bounds as follows:

$h^2 = 2d$:	2	4	6	8
$\max \#_\Sigma$:	72	144	36	56

9.1. **Double planes.** Any degree 2 model is hyperelliptic: $X \to \mathbb{P}^2$ is the double plane ramified over a smooth sextic curve $C \subset \mathbb{P}^2$. The projection establishes a two-to-one correspondence between lines on X and tritangents to C and, essentially by the definition, an h-fragment is the pair of lines over a tritangent. That is, we always have $\#_\Sigma(X) = \frac{1}{2}|\operatorname{Fn} X|$. According to [4, Addendum 1.2], this number takes values $\{0..66, 72\}$ except, possibly, 61.

9.2. **Double quadrics.** A hyperelliptic quartic $X \to \mathbb{P}^1 \times \mathbb{P}^1 \hookrightarrow \mathbb{P}^2$ is a double quadric ramified over a smooth curve $C \subset \mathbb{P}^1 \times \mathbb{P}^1$ of bi-degree $(4,4)$. Lines on X are in a two-to-one correspondence with the generatrices of the quadric bitangent to C, and an h-fragment is the pull-back of a pair of intersecting bitangents. It follows that $\#_\Sigma = n_1 n_2$, where n_i is the number of bitangents in the i-th ruling of the quadric, $i = 1, 2$. We have $n_i \leqslant 12$, and found in [3, Corollary 1.4] is an example of a quartic with $n_1 = n_2 = 12$. Hence, the sharp upper bound is $\#_\Sigma(X) \leqslant 144$.

9.3. **Sextics and octics.** A hyperelliptic $K3$-surface $X \to Y \hookrightarrow \mathbb{P}^{d+1}$ of degree $2d = 6$ or 8 is a double scroll ramified over a certain smooth curve $C \subset Y$. (We do not consider the Veronese octic $X \to \mathbb{P}^2 \hookrightarrow \mathbb{P}^5$ as it has no lines.) The structure of the graph $\operatorname{Fn} X$ is described in [2, § 5.5]: there are

- a pair of lines ℓ_1, ℓ_2 over the exceptional section $E \subset Y$ (the circled vertices in Figure 4), so that $\ell_1 \cdot \ell_2 = 1$ if $2d = 6$ and $\ell_1 \cdot \ell_2 = 1$ if $2d = 8$, and
- a certain number n of pairwise disjoint $\tilde{\mathbf{A}}_1$-fragments $\{m_{i1}, m_{i2}\}$, one over each bitangent to C, so that $m_{i1} \cdot m_{i2} = 2$ and $m_{ir} \cdot \ell_r = \delta_{rs}$.

We have $n \leqslant 9$ if $2d = 6$ and $n \leqslant 8$ if $2d = 8$.

Remark 9.1. In [2] it is stated that $n \leqslant 10$ if $2d = 6$ and $n \leqslant 12$ if $2d = 8$. These values can be attained only if the two lines ℓ_1, ℓ_2 over E are not present. If they are present, the graph is 1-admissible but not geometric for $2d = 6$ and $10 \leqslant n \leqslant 12$, and it is not even hyperbolic for $2d = 6$ and $n \geqslant 13$ or $2d = 8$ and $n \geqslant 9$.

A split hyperplane section on X is the pull-back of a hyperplane section of Y split into E and $(d-1)$ bitangents. Since there is a unique d-plane in $\mathbb{P}^{d+1}$ through the line E and any $(d-1)$ fibers of the ruling, the possible counts are the binomial coefficients $C(m, d-1)$, $m \leqslant n$, *i.e.*,

$$\#_\Sigma(X) \in \begin{cases} \{0, 1, 3, 6, 10, 15, 21, 28, 36\}, & \text{if } 2d = 6, \\ \{0, 1, 4, 10, 20, 35, 56\}, & \text{if } 2d = 8. \end{cases}$$

References

1. Arnaud Beauville, *Application aux espaces de modules*, Astérisque **126** (1985), 141–152, Geometry of $K3$ surfaces: moduli and periods (Palaiseau, 1981/1982). MR 785231
2. Alex Degtyarev, *Lines on Smooth Polarized K3-Surfaces*, Discrete Comput. Geom. **62** (2019), no. 3, 601–648. MR 3996938
3. ———, *Smooth models of singular $K3$-surfaces*, Rev. Mat. Iberoam. **35** (2019), no. 1, 125–172. MR 3914542
4. ———, *Tritangents to smooth sextic curves*, Ann. Inst. Fourier (Grenoble) **72** (2022), no. 6, 2299–2338. MR 4500357
5. Alex Degtyarev, Igor Dolgachev, and Shigeyuki Kondō, *K3 surfaces of degree six arising from desmic tetrahedra*, To appear in Rendiconti Lincei. Matematica e Applicazioni, 2025.
6. Alex Degtyarev, Ilia Itenberg, and Ali Sinan Sertöz, *Lines on quartic surfaces*, Math. Ann. **368** (2017), no. 1-2, 753–809. MR 3651588
7. Alex Degtyarev and Sławomir Rams, *Extended Fano graphs of octic $K3$-surfaces*, Electronic, `http://www.fen.bilkent.edu.tr/~degt/papers/octics_Fano.zip`, March 2021.
8. ———, *Counting lines with Vinberg's algorithm*, To appear in Rev. Mat. Iberoam., 2025.
9. ———, *Lines on $K3$-quartics via triangular sets*, Discrete Comput. Geom. **73** (2025), no. 3, 785–814. MR 4880184
10. ———, *Lines on sextic $K3$-surfaces with simple singularities*, To appear, 2025.
11. The GAP Group, *GAP – Groups, Algorithms, and Programming, Version 4.13.0*, 2024.
12. Vik. S. Kulikov, *Surjectivity of the period mapping for $K3$ surfaces*, Uspehi Mat. Nauk **32** (1977), no. 4(196), 257–258. MR 0480528 (58 #688)
13. V. V. Nikulin, *Integer symmetric bilinear forms and some of their geometric applications*, Izv. Akad. Nauk SSSR Ser. Mat. **43** (1979), no. 1, 111–177, 238, English translation: Math USSR-Izv. 14 (1979), no. 1, 103–167 (1980). MR 525944 (80j:10031)
14. I. I. Pjateckiĭ-Šapiro and I. R. Šafarevič, *Torelli's theorem for algebraic surfaces of type* K3, Izv. Akad. Nauk SSSR Ser. Mat. **35** (1971), 530–572, English translation: Math. USSR-Izv. 5, 547–588. MR 0284440 (44 #1666)
15. Sławomir Rams and Matthias Schütt, *On quartics with lines of the second kind*, Adv. Geom. **14** (2014), no. 4, 735–756. MR 3276131
16. Sławomir Rams and Matthias Schütt, *64 lines on smooth quartic surfaces*, Math. Ann. **362** (2015), no. 1-2, 679–698. MR 3343894
17. B. Saint-Donat, *Projective models of K-3 surfaces*, Amer. J. Math. **96** (1974), 602–639. MR 0364263 (51 #518)
18. Friedrich Schur, *Ueber eine besondre Classe von Flächen vierter Ordnung*, Math. Ann. **20** (1882), no. 2, 254–296. MR 1510168
19. B. Segre, *The maximum number of lines lying on a quartic surface*, Quart. J. Math., Oxford Ser. **14** (1943), 86–96. MR 0010431 (6,16g)

DEPARTMENT OF MATHEMATICS, BILKENT UNIVERSITY, 06800 ANKARA, TURKEY
Email address: `degt@fen.bilkent.edu.tr`